Biochemical and Biophysical Research Communications 435 (2013) 113–119

Contents lists available at SciVerse ScienceDirect

Biochemical and Biophysical Research Communications

journal homepage: www.elsevier.com/locate/ybbrc

# Small GTPase Rab39A interacts with UACA and regulates the retinoic acid-induced neurite morphology of Neuro2A cells

Yasunori Mori, Takahide Matsui, Daisuke Omote, Mitsunori Fukuda *

*Laboratory of Membrane Trafficking Mechanisms, Department of Developmental Biology and Neurosciences, Graduate School of Life Sciences, Tohoku University, Aobayama, Aoba-ku, Sendai, Miyagi 980-8578, Japan*

ARTICLE INFO

*Article history:*
Received 4 April 2013
Available online 23 April 2013

*Keywords:*
Rab39 effector
Small GTPase
Membrane traffic
Neuro2A cells
Neuritogenesis
UACA

ABSTRACT

We screened for a Rab39-specific effector by performing a yeast two-hybrid assay with GTP-locked Rab39A/B as the bait and identified UACA (uveal autoantigen with coiled-coil domains and ankyrin repeats) as a specific Rab39A/B-binding protein. Deletion analysis revealed that a C-terminal coiled-coil domain of UACA functions as a GTP-dependent Rab39-binding domain. shRNA-mediated knockdown of endogenous Rab39A or UACA in mouse neuroblastoma Neuro2A cells resulted in a change in retinoic acid-induced neurite morphology from a multipolar morphology to a bipolar morphology. Taken together, these findings indicate that UACA functions as a Rab39A effector in the retinoic acid-induced differentiation of Neuro2A cells.



## 1. Introduction

Rab small GTPases are conserved membrane trafficking proteins in all eukaryotes, and they regulate a variety of steps in membrane traffic, including vesicle budding, vesicle movement along the cytoskeleton, vesicle docking to specific membranes, and vesicle fusion [1,2]. Rab functions as a molecular switch by cycling between a GDP-bound inactive state (OFF state) and a GTP-bound active state (ON state), and the GTP-bound active form mediates membrane traffic through interaction with a specific effector molecule [3,4]. Approximately 60 distinct Rab isoforms have been identified in mammals [5], and each isoform is thought to regulate a specific step(s) or specific type(s) of membrane traffic. However, since the exact function of most mammalian Rabs, especially of mammalian specific Rabs, largely remains unknown, identification of the specific effector molecules for each Rab isoform is one of the most important steps toward understanding the molecular mechanisms of Rab-mediated membrane traffic in mammals. Several attempts to comprehensively screen for mammalian Rab effectors have been made recently [6,7], but the specific effector molecules for most Rabs remain to be determined.

Rab39 is a less well characterized Rab isoform that is conserved in most metazoans [5]. Two Rab39 isoforms, Rab39A and Rab39B, are present in humans and mice, and they share 78% amino acid identity [8,9]. Rab39A is widely expressed in a variety of tissues, while Rab39B is specifically expressed in the neurons of mouse and human brain [10,11]. It has been reported that Rab39A binds caspase-1 and regulates lipopolysaccharide-induced secretion of IL-1β in thymocytes [12] and that Rab39B is associated with X-linked mental retardation and is involved in maintenance of neurite morphology and synapse [10]. More recently, *Caenorhabditis elegans* RAB-39 has been shown to be involved in the oxidative stress response possibly through interaction with RASF-1, a homologue of Ras association domain family [13]. However, the molecular basis of the role of mammalian Rab39 in membrane traffic is not fully understood.

In this study, we screened for a Rab39-specific effector by performing a yeast two-hybrid assay, and the results showed that UACA (uveal autoantigen with coiled-coil domains and ankyrin repeats; also known as Nucling [14]) functions as a Rab39A/B-specific binding protein. In addition, knockdown of either Rab39A or UACA in retinoic acid (RA)-differentiated Neuro2A cells induced a change in cell morphology from a multipolar cell to a bipolar morphology. We discuss the possible function of UACA as an effector molecule of Rab39 based on our findings.

*Abbreviations:* aa, amino acid residues; CA/CN, constitutive active/negative; CC, coiled-coil; EGFP, enhanced green fluorescent protein; RA, retinoic acid; shRNA, short hairpin RNA; SR, shRNA-resistant; mStr, monomeric Strawberry; UACA, uveal autoantigen with coiled-coil domains and ankyrin repeats.

* Corresponding author. Fax: +81 22 795 7733.
*E-mail address:* nori@m.tohoku.ac.jp (M. Fukuda).

0006-291X/$ - see front matter © 2013 Elsevier Inc. All rights reserved.
http://dx.doi.org/10.1016/j.bbrc.2013.04.051

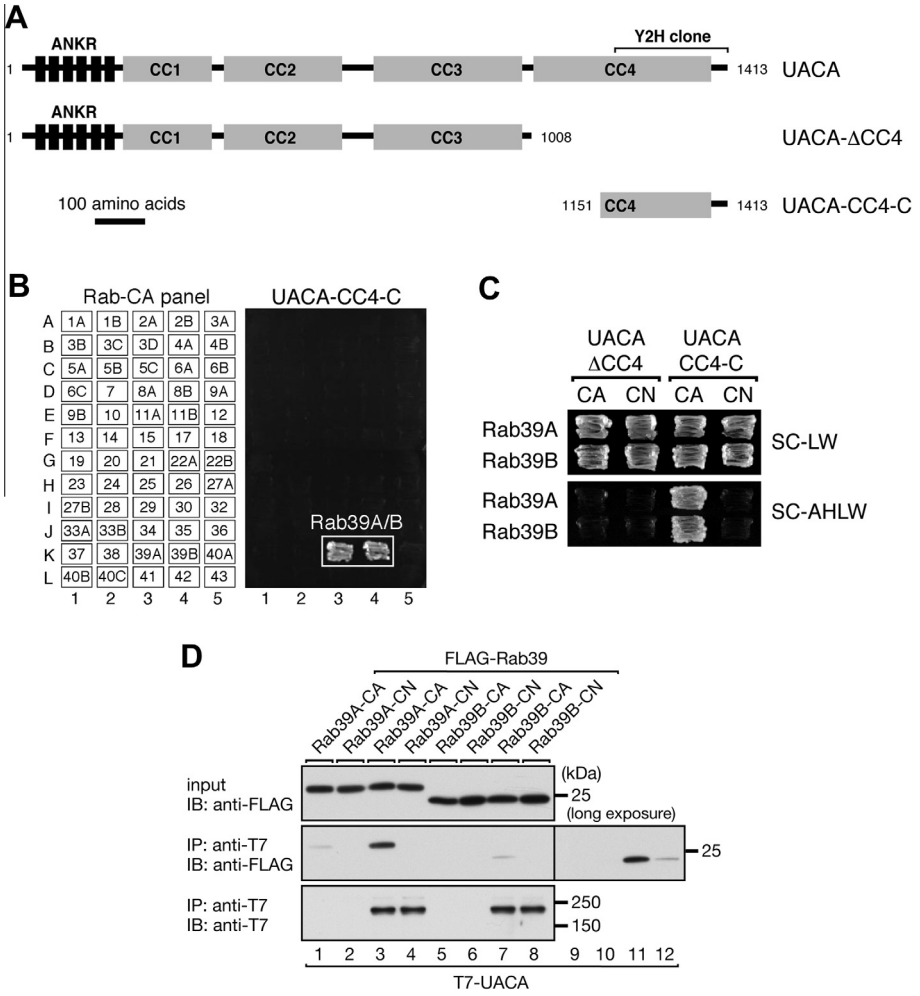


**Fig. 1.** UACA functions as a Rab39-specific binding protein. (A) Schematic representation of UACA and the truncated UACA mutants used in this study. UACA consists of an ankyrin repeat (ANKR) domain and four coiled-coil domains (CC1-CC4). (B) Specific interaction between UACA and the GTP-fixed form of Rab39A/B. Yeast cells containing pGBD plasmid expressing constitutive active (CA, GTP-locked) Rab protein (positions indicated in the left panel) and pAct2 plasmid expressing the C-terminal fragment of UACA (aa 1181-1413) were streaked on SC-AHLW medium and incubated at 30 °C. (C) GTP-dependent interaction between UACA-CC4-C and Rab39A/B. Yeast cells containing pGBD-C1-Rab39A/B(CA/CN) and pAct2-UACA-ΔCC4 or pAct2-UACA-CC4-C were streaked on SC-LW medium and SC-AHLW medium and incubated at 30 °C. (D) Interaction between T7-UACA and FLAG-Rab39A/B(CA/CN) in COS-7 cells. Note that UACA appeared to bind Rab39A more preferably than Rab39B in COS-7 cells. Lanes 9–12 correspond to the long exposure data on lanes 5–8 in the middle panel.

## 2. Materials and methods

### 2.1. Antibodies

Anti-Rab39 and anti-UACA rabbit polyclonal antibodies were raised against glutathione *S*-transferase (GST)-Rab39B [15] and GST-UACA-N (amino acid residues (aa) 1-251) as described previously [16].

### 2.2. Plasmid construction

cDNAs of the constitutive active (CA,GTP-fixed) mutants of Rab39A(Q72L) lacking the C-terminal geranylgeranylation site (ΔCys) and Rab39B(Q68L)ΔCys or constitutive negative (CN, GDP-fixed) mutants of Rab39A(S22N)ΔCys and Rab39B(S22N)ΔCys were subcloned into the pGBD-C1 vector as described previously [6,17]. The mouse UACA cDNA (UACA-full; aa 1-1413) was amplified from Marathon-Ready mouse brain cDNA (Clontech-Takara Bio Inc., Shiga, Japan) by PCR with specific pairs of oligonucleotides as described previously [18], and their sequences are available from the authors on request. Truncated mutants of UACA, i.e., UACA-N (aa 1-251), UACA-ΔCC4 (aa 1-1008), and UACA-CC4-C (aa 1151-1413), were constructed by conventional PCR techniques. The cDNAs of full-length UACA and the truncated mutants of UACA were subcloned into pAct2 (Clontech-Takara Bio Inc.), pGEX-4T-3 (GE Healthcare, Chalfont St. Giles, Buckinghamshire, UK), pEGFP-C1 (Clontech-Takara Bio Inc.) and/or pEF-T7 tag expression vector [18]. pEF-FLAG-Rab39A and pEF-FLAG-Rab39B were prepared as described previously [19,20]. The cDNAs of Rab39A and Rab39B were subcloned into pGEX-4T-3, pEGFP-C1, and/or pmStrawberry-C1 (pmStr-C1) [21]. pSilencer-CMV-EGFP (enhanced green fluorescent protein) vector (or pSilencer-CMV-mStr vector) was generated from pSilencer 2.1-U6 neo vector (pSilencer-neo; Ambion, Austin, TX) by substituting the SspI insert of pSilencer-neo for the CMV promoter-EGFP region (or CMV promoter-mStrawberry region), which had been amplified by PCR with the following primers by using pEGFP-C1 (or pmStr-C1) as a template: 5′-AGTAATCAA TTACGGGGTC-3′ and 5′-GCGTTAAGATACATTGATGAG-3′. pSilencer-neo, pSilencer-CMV-EGFP, and pSilencer-CMV-mStr vectors expressing mouse *Rab39A*-short hairpin RNA (shRNA) (19-base target site: 5′-CATGTGAAAGATTGGCTAG-3′), *Rab39B*-shRNA (19-base

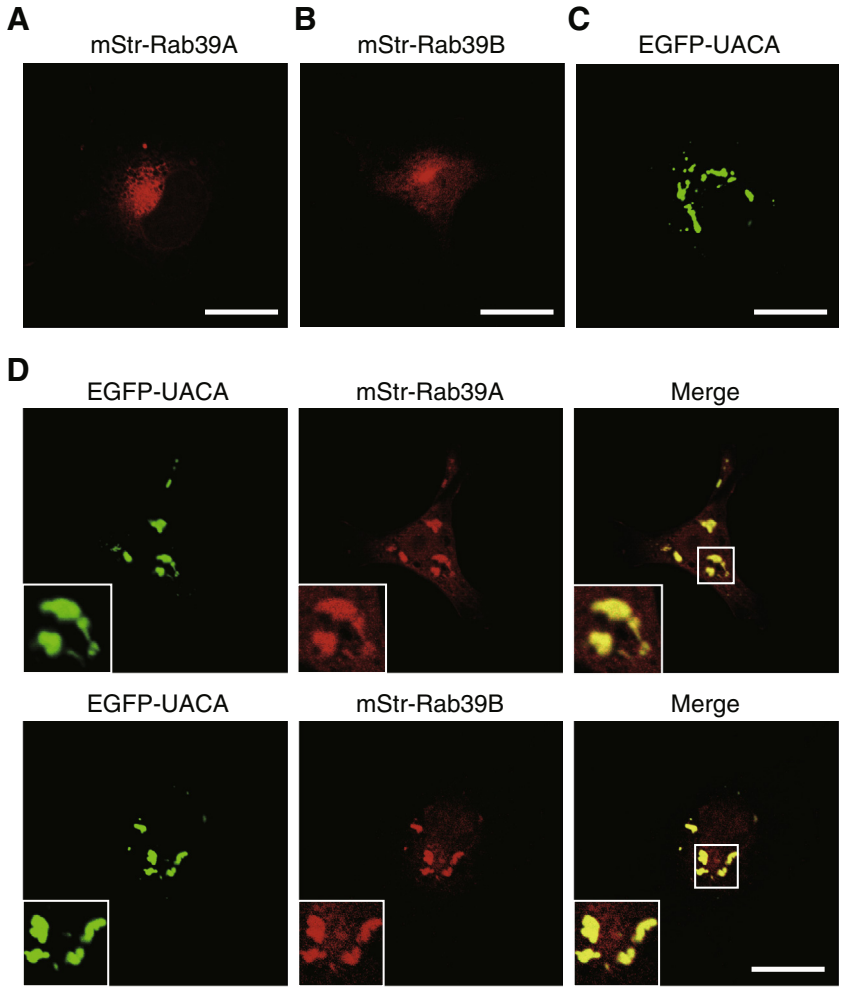


**Fig. 2.** UACA colocalizes with Rab39A/B in COS-7 cells. (A-C) COS-7 cells were transfected with pmStr-C1-Rab39A (A), pmStr-C1-Rab39B (B), or pEGFP-C1-UACA (C) alone, and the cells were fixed one day after transfection. (D) COS-7 cells were cotransfected with pEGFP-C1-UACA and pmStr-C1-Rab39A (upper panels) or with pmStr-C1-Rab39B (lower panels) and the cells were fixed one day after transfection. The insets show magnified views of the boxed area. Bars, 20 μm.

target site: 5′-ATCAGAGAGGAGATGTTTG-3′), and *UACA*-shRNA (19-base target site: 5′-CTGAAAATGAGATTTTAAA-3′) were prepared as described previously [22]. pEGFP-C1-Rab39A$^{SR}$, pMyc-Rab39A$^{SR}$ and pEGFP-C1-UACA$^{SR}$ (shRNA-resistant Rab39A and UACA mutants) were produced by a two-step PCR technique as described previously [23], and their sequences are also available from the authors on request.

### 2.3. Yeast two-hybrid assays

The yeast strain (pJ69-4A), SC-LW medium (synthetic complete medium lacking leucine and tryptophan), selection medium SC-AHLW (synthetic complete medium lacking adenine, histidine, leucine, and tryptophan), culture conditions, and transformation protocol used are described in James et al. [24]. pGBD-C1-Rab39A(Q72L)ΔCys and pGBD-C1-Rab39B(Q68L)ΔCys [19] were used as bait to screen oligo(dT)-primed mouse testis and mouse embryo mixed cDNA libraries according to the manufacturer's instructions (Clontech-Takara Bio Inc.), and $1 \times 10^8$ colonies were investigated [6].

### 2.4. Cell cultures and transfections

COS-7 cells and Neuro2A cells were cultured in Dulbecco's modified Eagle medium (DMEM) supplemented with 10% fetal bovine serum, 50 U/ml penicillin, and 50 U/ml streptomycin. The cells were plated onto a 6-well or 12-well plate(s). Plasmid DNAs were transfected into COS-7 and Neuro2A cells by using LipofectAMINE Plus and LipofectAMINE 2000 (Invitrogen, Carlsbad, CA), respectively.

### 2.5. Binding assays

Coimmunoprecipitation assays in COS-7 cells were performed essentially as described previously [18,25].

### 2.6. RA-induced neuritogenesis of Neuro2A cells

Differentiation of Neuro2A cells was induced with RA as described previously with slight modifications [26]. In brief, one day after transfection the cells were treated with 2 μM RA (Sigma–Aldrich, St. Louis, MO) in DMEM containing 2% fetal bovine serum. Two days later the cells were fixed in 4% paraformaldehyde in 0.1 M sodium phosphate buffer and examined for fluorescence of EGFP or mStr with a confocal fluorescence microscope (Fluoview 1000; Olympus, Tokyo, Japan). We classified Neuro2A cells having one or more neurites extending more than 10 μm from the cell body as differentiated cells and counted the number of multipolar cells (3 or more neurites) and bipolar cells (1–2 neurites) ($n > 150$ in three independently prepared dishes). Total neurite numbers

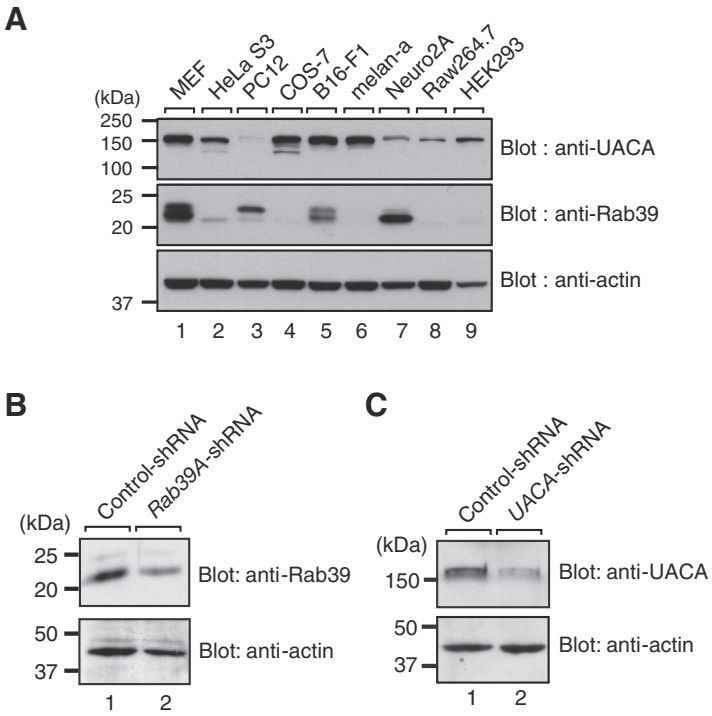


**Fig. 3.** Expression profiles of UACA and Rab39A/B in mammalian cell lines. (A) Lysates of the cells indicated were analyzed by immunoblotting with the antibodies indicated. The doublet bands detected by anti-Rab39 antibody (e.g., lanes 1 and 5) presumably correspond to Rab39A and Rab39B. (B) and (C) Knockdown efficiency of *Rab39A*-shRNA and *UACA*-shRNA in Neuro2A cells. Neuro2A cells were transfected with pSilencer-neo-Control (lane 1), pSilencer-neo-Rab39A (lane 2 in B), or pSilencer-neo-UACA (lane 2 in C). Two days after transfection the cells were lysed and the lysates were subjected to immunoblot analysis with the antibodies indicated.

and total neurite length were determined manually by using the ImageJ software. The proportion (%) of bipolar cells was calculated by dividing the number of bipolar cells by the total number of differentiated cells (bipolar cells plus multipolar cells).

### 2.7. Immunocytochemistry

Cells were fixed for 10 min at room temperature with 4% paraformaldehyde (Wako Pure Chemical Industries, Osaka, Japan), permeabilized with 0.3% Triton X-100 for 2 min, and then stained with specific antibodies. The cells were examined for fluorescence with the confocal fluorescence microscope, and the images were processed with Adobe Photoshop software (CS4).

### 2.8. Statistical analysis

The results in Figs. 4B–E are shown as the mean value and SEM ($n > 150$). Values were analyzed for statistically significant differences by Tukey's multiple comparison test. A $p$ value of $< 0.05$ was considered statistically significant. All statistical analyses were performed on data obtained from three independent experiments.

## 3. Results

### 3.1. Identification of UACA as a Rab39A/B-specific binding protein

To identify a novel Rab39A/B-specific effector molecule(s), we screened mouse cDNA libraries by performing yeast two-hybrid assays with the constitutive active (CA, GTP-fixed) form of Rab39A/B as bait. Using Rab39B as bait enabled us to identify a clone that encodes the C-terminal fragment of UACA (aa 1181-1413) (Fig. 1A). A yeast two-hybrid assay with a panel of 60 different GTP-locked Rabs [6] revealed that UACA-CC4-C, which contains the C-terminal half of the coiled-coil 4 (CC4) domain, interacted with Rab39A and Rab39B alone (Fig. 1B), and UACA-CC4-C, but not UACA-ΔCC4, specifically interacted with the CA form of Rab39A/B, but not with their CN form (Fig. 1C), indicating that UACA-CC4-C is necessary and sufficient for specific recognition of the active Rab39. Moreover, coimmunoprecipitation assays showed that the GTP-dependent Rab39A/B–UACA interaction also occurred in cultured mammalian cells (Fig. 1D, middle).

### 3.2. Colocalization between UACA and Rab39A/B

If UACA functions as a Rab39 effector, UACA and Rab39A should be colocalized in cultured cells. Because the antibodies against UACA and Rab39 that we prepared for use in this study (see next section below) failed to work in an immunofluorescence analysis, we coexpressed EGFP-tagged UACA and mStr-tagged Rab39A (or Rab39B) in COS-7 cells and investigated their subcellular localization by confocal fluorescence microscopy. Consistent with a previous observation [10], both mStr-Rab39A and mStr-Rab39B were seen to mainly be localized in the Golgi region when they were expressed alone in COS-7 cells (Fig. 2A and B, and Supplementary Fig. S1A), whereas EGFP-UACA was localized at unidentified dot-like structures (Fig. 2C) that were negative for all of the organelle markers tested, including Golgi, *trans*-Golgi network, endoplasmic reticulum, endosome, and lysosome markers (Supplementary Fig. S1B). Intriguingly, however, when EGFP-UACA and mStr-Rab39A/B were coexpressed in COS-7 cells they were observed to be colocalized at the dot-like structures outside the Golgi region (Fig. 2D and Supplementary Fig. S1C). Taken together, these findings indicated that UACA is a plausible candidate for Rab39-specific effector in mammalian cells.

### 3.3. Involvement of Rab39A and UACA in RA-induced differentiation of Neuro2A cells

Next, we tested nine cultured mammalian cell lines for endogenous expression of UACA and Rab39A/B by immunoblotting with

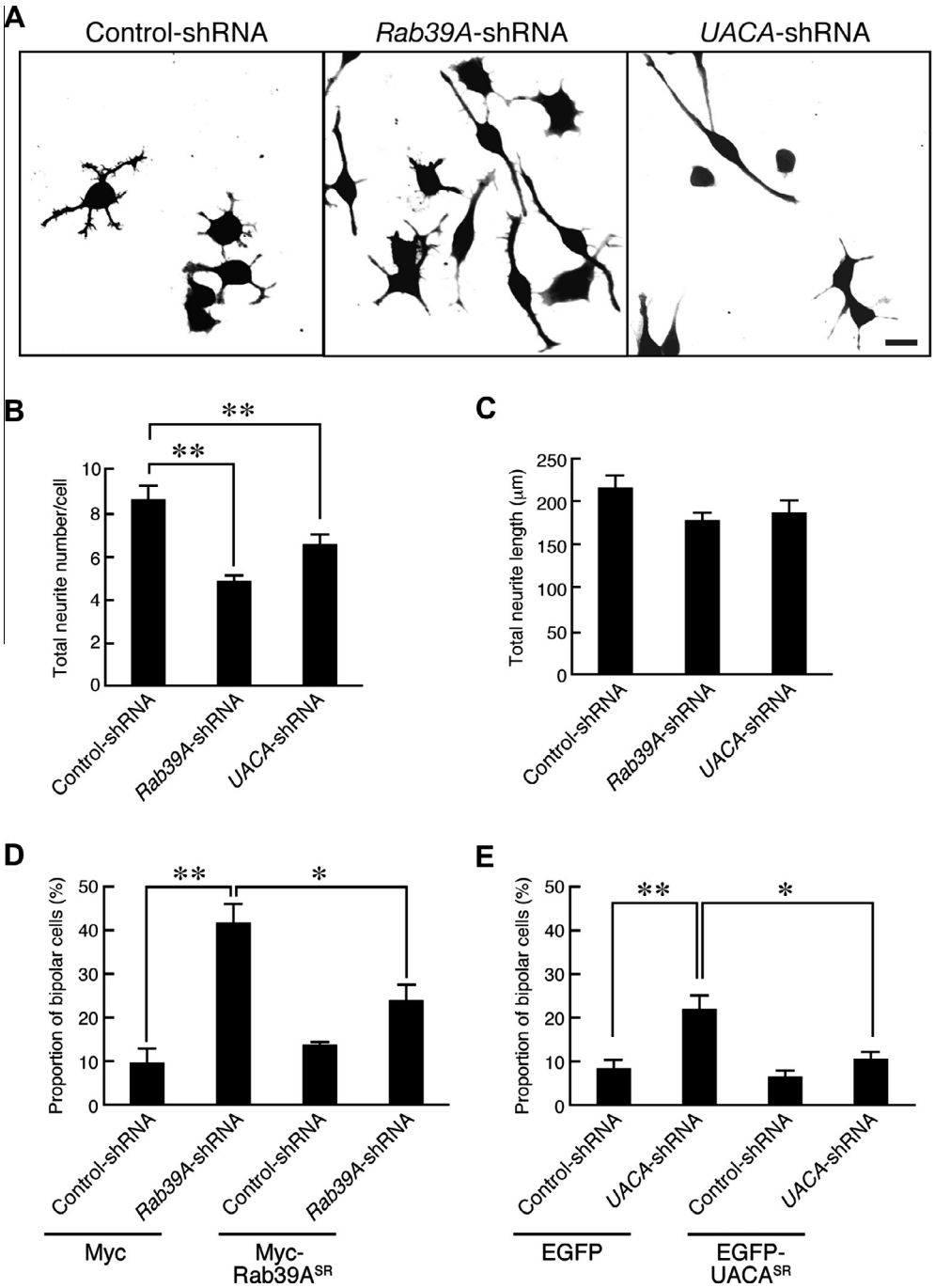


**Fig. 4.** Rab39A and UACA are involved in RA-induced neuritogenesis of Neuro2A cells. (A) Typical images of RA-differentiated Neuro2A cells in the presence of the shRNAs indicated. The cells in the EGFP fluorescence image (i.e., shRNA-expressing cells) are shown in black. Bar, 50 μm. (B and C) Quantification of total neurite numbers (B) and total neurite length (C) shown in (A). ** $p < 0.01$. (D and E) Quantification of the proportion of RA-differentiated Neuro2A cells having a bipolar morphology. (D) Neuro2A cells were transfected with pSilencer-CMV-mStr-Control or pSilencer-CMV-mStr-Rab39A together with pMyc-Control or pMyc-Rab39A$^{SR}$. (E) Neuro2A cells were transfected with pSilencer-CMV-mStr-Control or pSilencer-CMV-mStr-UACA together with pEGFP-C1 or pEGFP-C1-UACA$^{SR}$. (A-E) Two days after treatment with RA, the cells were fixed and examined with a confocal fluorescence microscope. The proportion (%) of Neuro2A cells having a bipolar morphology was calculated as described in the Materials and methods section. ** $p < 0.01$; * $p < 0.05$.

specific antibodies. As shown in Fig. 3A (top), the anti-UACA antibody specifically recognized 150-kDa bands that closely matched the estimated molecular mass of UACA, and abundant expression of the molecule was observed in every cell line except PC12 cells. By contrast, the anti-Rab39 antibody, which recognized both Rab39A and Rab39B (data not shown), detected a single band or doublet bands around 22-kDa in certain cell lines. Abundant Rab39 expression was found in MEF, PC12, B16-F1, and Neuro2A cells, but only a trace amount of Rab39 or virtually no expression of Rab39 was observed in any of the other cell lines (Fig. 3A, middle).

We selected one of the cell lines tested, Neuro2A cells, for subsequent analysis of the functional relationship between Rab39 and UACA for two reasons. Our first reason was that Rab39B has been shown to be involved in neuritogenesis of cultured hippocampal neurons [10], and Neuro2A cells are known to extend neurites in response to RA [26]. Our second reason was that Neuro2A cells

express both UACA and a single band (or isoform) of Rab39, and they can easily be used for RNA interference-mediated knockdown experiments [27]. We generated specific shRNAs against Rab39A, Rab39B, and UACA and their shRNA-resistant mutants (Supplementary Figs. S2A, S2B, and S3A) and attempted to evaluate the knockdown effect of shRNAs on RA-induced neuritogenesis. The *UACA*-shRNA and *Rab39A*-shRNA we produced clearly decreased the intensity of the immunoreactive bands around 150-kDa and 22-kDa, respectively, confirming the specificity of the shRNAs (Fig. 3B and C). When Neuro2A cells were treated for 2 days with RA, the cells often extended more than 3 neurites (multipolar cell morphology; see Fig. 4A, left) as described previously [26]. Unexpectedly, Neuro2A cells extended neurites even in the absence of Rab39A or UACA. Intriguingly, however, knockdown of either Rab39A or UACA resulted in a significant increase in the proportion of bipolar cells that extended 1–2 neurites from the cell body (Fig. 4A, middle and right) and a significant decrease in the numbers of neurites (Fig. 4B) without altering total neurite length (Fig. 4C). By contrast, the *Rab39B*-shRNA had no effect on the morphology of RA-differentiated Neuro2A cells (Supplementary Fig. S3B and S3C), suggesting that Neuro2A cells predominantly express Rab39A rather than Rab39B. This morphological change cannot have been attributable to an off-target effect of the shRNAs, because re-expression of an shRNA-resistant Rab39A$^{SR}$ mutant in Rab39A-knockdown cells significantly decreased the proportion of bipolar cells (Fig. 4D). Similarly, re-expression of UACA$^{SR}$ in UACA-knockdown cells completely restored their multipolar morphology (Fig. 4E). These results indicated that both Rab39A and UACA are involved in RA-induced differentiation of Neuro2A cells, especially in the process of multiple neurite formation (i.e., multipolar morphology).

## 4. Discussion

Several functions of Rab39 have been reported previously [10,12,13], but the molecular basis of the role of Rab39 in membrane traffic is not fully understood. In the present study, we have presented several lines of evidence showing that UACA is a plausible candidate for a Rab39 effector in mammals. First, we identified UACA as a GTP-Rab39A/B-specific binding protein and mapped its binding site to the C-terminal region of the CC4 domain (Fig. 1). Although several Rab39-binding proteins have been identified [7,12,13], UACA is the only Rab39-binding protein whose Rab binding specificity has been precisely determined, because UACA was shown to interact exclusively with Rab39A/B and not to interact with 58 other Rabs (Fig. 1B). Second, we demonstrated that EGFP-UACA and mStr-Rab39A/B are colocalized in COS-7 cells (Fig. 2D). Third, we found that both UACA and Rab39A are endogenously expressed in Neuro2A cells (Fig. 3) and that knockdown of either molecule in RA-differentiated Neuro2A cells causes a change in cell morphology from a multipolar morphology to a bipolar morphology (Fig. 4).

It has been reported that Rab39B is involved in the neuritogenesis of cultured mouse hippocampal neurons and that knockdown of Rab39B decreases the number of neuronal branches [10]. This phenotype closely resembles the bipolar morphology (i.e., decreased number of neurites) of Rab39A-knockdown Neuro2A cells in this study (Fig. 4A). Thus, it is tempting to speculate that both Rab39A and Rab39B have essentially the same ability to regulate neurite morphology and that both isoforms are differently expressed in mouse tissues or cells. Actually, Rab39B is predominant in mouse brain [10], whereas Rab39A seemed to be predominant in Neuro2A cells (Fig. 3B). We also demonstrated that knockdown of UACA phenocopies the Rab39A deficiency in RA-differentiated Neuro2A cells (Fig. 4D and E), although the effect of *UACA*-shRNA was weaker than that of *Rab39A*-shRNA. The weaker effect of *UACA*-shRNA may have been attributable to insufficient knockdown of endogenous UACA. Alternatively, another type of Rab39 effector molecule, e.g., caspase-1 [12] or RASSF-1 [13], may be involved in this process [28]. Since UACA is also expressed in mouse brain (our unpublished data), it is highly possible that UACA functions as a Rab39B effector during the process of neurite branching in hippocampal neurons. Further research will be necessary to determine whether UACA is actually involved in the regulation of neuritogenesis and/or synapse formation by neurons in the same way as Rab39B is [10].

UACA was originally identified as an autoantigen in patients with panuveitis [29] and it has been shown to be associated with myocardial differentiation [14] and apoptosis [30,31], but involvement of Rab39 in these cellular functions has never been investigated. However, since Rab39A physically interacts with caspase-1 [12], it will be very interesting to determine whether the Rab39–UACA complex is also involved in myocardial differentiation and apoptosis in the future.

In summary, we have identified UACA as a Rab39A/B-specific binding protein and demonstrated that knockdown of endogenous Rab39A or UACA in RA-differentiated Neuro2A cells changed their morphology from a multipolar morphology to a bipolar morphology. We propose that UACA functions as a specific Rab39 effector molecule that regulates the branching or formation of neurites, possibly by promoting membrane traffic from the Golgi, where Rab39 is usually present (Fig. 2A and B) [10], to neurites.

## Acknowledgments

This work was supported in part by Grants-in-Aid for Scientific Research from the Ministry of Education, Culture, Sports, and Technology (MEXT) of Japan (to Y. M., and M. F.) and by a grant from the Daiichi-Sankyo Foundation of Life Science (to M. F.). T. M. was supported by the Japan Society for the Promotion of Science (JSPS). We thank Megumi Aizawa for technical assistance and members of the Fukuda Laboratory for valuable discussions.

## Appendix A. Supplementary data

Supplementary data associated with this article can be found, in the online version, at http://dx.doi.org/10.1016/j.bbrc.2013.04.051.

## References

[1] M. Fukuda, Regulation of secretory vesicle traffic by Rab small GTPases, Cell. Mol. Life Sci. 65 (2008) 2801–2813.
[2] H. Stenmark, Rab GTPases as coordinators of vesicle traffic, Nat. Rev. Mol. Cell Biol. 10 (2009) 513–525.
[3] B.L. Grosshans, D. Ortiz, P. Novick, Rabs and their effectors: achieving specificity in membrane traffic, Proc. Natl. Acad. Sci. USA 103 (2006) 11821–11827.
[4] S.L. Schwartz, C. Cao, O. Pylypenko, A. Rak, A. Wandinger-Ness, Rab GTPases at a glance, J. Cell Sci. 120 (2007) 3905–3910.
[5] Y. Diekmann, E. Seixas, M. Gouw, F. Tavares-Cadete, M.C. Seabra, J.B. Pereira-Leal, Thousands of rab GTPases for the cell biologist, PLoS Comput. Biol. 7 (2011) e1002217.
[6] M. Fukuda, E. Kanno, K. Ishibashi, T. Itoh, Large scale screening for novel Rab effectors reveals unexpected broad Rab binding specificity, Mol. Cell. Proteomics 7 (2008) 1031–1042.
[7] E. Kanno, K. Ishibashi, H. Kobayashi, T. Matsui, N. Ohbayashi, M. Fukuda, Comprehensive screening for novel Rab-binding proteins by GST pull-down assay using 60 different mammalian Rabs, Traffic 11 (2010) 491–507.
[8] T. Stankovic, P.J. Byrd, P.R. Cooper, C.M. McConville, D.J. Munroe, J.H. Riley, G.D.J. Watts, H. Ambrose, G. McGuire, A.D. Smith, A. Sutcliffe, T. Mills, A.M.R. Taylor, Construction of a transcription map around the gene for ataxia telangiectasia: identification of at least four novel genes, Genomics 40 (1997) 267–276.
[9] H. Cheng, Y. Ma, X. Ni, M. Jiang, L. Guo, K. Ying, Y. Xie, Y. Mao, Isolation and characterization of a human novel RAB (RAB39B) gene, Cytogenet. Genome Res. 97 (2002) 72–75.

[10] M. Giannandrea, V. Bianchi, M.L. Mignogna, A. Sirri, S. Carrabino, E. D'Elia, M. Vecellio, S. Russo, F. Cogliati, L. Larizza, H.H. Ropers, A. Tzschach, V. Kalscheuer, B. Oehl-Jaschkowitz, C. Skinner, C.E. Schwartz, J. Gecz, H. Van Esch, M. Raynaud, J. Chelly, A.P.M. de Brouwer, D. Toniolo, P. D'Adamo, Mutations in the small GTPase gene *RAB39B* are responsible for X-linked mental retardation associated with autism, epilepsy, and macrocephaly, Am. J. Hum. Genet. 86 (2010) 185–195.
[11] T. Chen, Y. Han, M. Yang, W. Zhang, N. Li, T. Wan, J. Guo, X. Cao, Rab39, a novel Golgi-associated Rab GTPase from human dendritic cells involved in cellular endocytosis, Biochem. Biophys. Res. Commun. 303 (2003) 1114–1120.
[12] C.E. Becker, E.M. Creagh, L.A.J. O'Neill, Rab39a binds caspase-1 and is required for caspase-1-dependent interleukin-1β secretion, J. Biol. Chem. 284 (2009) 34531–34537.
[13] M. Takenaka, H. Inoue, A. Takeshima, T. Kakura, T. Hori, *C. elegans* Rassf homolog, *rasf-1*, is functionally associated with *rab-39* Rab GTPase in oxidative stress response, Genes Cells 18 (2013) 203–210.
[14] T. Sakai, L. Liu, Y. Shishido, K. Fukui, Identification of a novel, embryonal carcinoma cell-associated molecule, nucling, that is up-regulated during cardiac muscle differentiation, J. Biochem. 133 (2003) 429–436.
[15] T. Itoh, N. Fujita, E. Kanno, A. Yamamoto, T. Yoshimori, M. Fukuda, Golgi-resident small GTPase Rab33B interacts with Atg16L and modulates autophagosome formation, Mol. Biol. Cell 19 (2008) 2916–2925.
[16] M. Fukuda, K. Mikoshiba, A novel alternatively spliced variant of synaptotagmin VI lacking a transmembrane domain: implications for distinct functions of the two isoforms, J. Biol. Chem 274 (1999) 31428–31434.
[17] M. Fukuda, H. Kobayashi, K. Ishibashi, N. Ohbayashi, Genome-wide investigation of the Rab binding activity of RUN domains: development of a novel tool that specifically traps GTP-Rab35, Cell Struct. Funct. 36 (2011) 155–170.
[18] M. Fukuda, E. Kanno, K. Mikoshiba, Conserved N-terminal cysteine motif is essential for homo- and heterodimer formation of synaptotagmins III, V, VI, and X, J. Biol. Chem. 274 (1999) 31421–31427.
[19] T. Itoh, M. Satoh, E. Kanno, M. Fukuda, Screening for target Rabs of TBC (Tre-2/Bub2/Cdc16) domain-containing proteins based on their Rab-binding activity, Genes Cells 11 (2006) 1023–1037.
[20] M. Fukuda, Distinct Rab binding specificity of Rim1, Rim2, rabphilin, and Noc2: identification of a critical determinant of Rab3A/Rab27A recognition by Rim2, J. Biol. Chem. 278 (2003) 15373–15380.
[21] N.C. Shaner, R.E. Campbell, P.A. Steinbach, B.N.G. Giepmans, A.E. Palmer, R.Y. Tsien, Improved monomeric red, orange and yellow fluorescent proteins derived from *Discosoma* sp. red fluorescent protein, Nat. Biotechnol. 22 (2004) 1567–1572.
[22] T.S. Kuroda, M. Fukuda, Rab27A-binding protein Slp2-a is required for peripheral melanosome distribution and elongated cell shape in melanocytes, Nat. Cell Biol. 6 (2004) 1195–1203.
[23] K. Tamura, N. Ohbayashi, K. Ishibashi, M. Fukuda, Structure-function analysis of VPS9-ankyrin-repeat protein (Varp) in the trafficking of tyrosinase-related protein 1 in melanocytes, J. Biol. Chem. 286 (2011) 7507–7521.
[24] P. James, J. Halladay, E.A. Craig, Genomic libraries and a host strain designed for highly efficient two-hybrid selection in yeast, Genetics 144 (1996) 1425–1436.
[25] T.S. Kuroda, M. Fukuda, Identification and biochemical analysis of Slac2-c/MyRIP as a Rab27A-, myosin Va/VIIa-, and actin-binding protein, Methods Enzymol. 403 (2005) 431–444.
[26] T.B. Shea, I. Fischer, V.S. Sapirstein, Effect of retinoic acid on growth and morphological differentiation of mouse NB2a neuroblastoma cells in culture, Brain Res. 353 (1985) 307–314.
[27] Y. Mori, T. Matsui, Y. Furutani, Y. Yoshihara, M. Fukuda, Small GTPase Rab17 regulates dendritic morphogenesis and postsynaptic development of hippocampal neurons, J. Biol. Chem. 287 (2012) 8963–8973.
[28] T. Vaisid, N.S. Kosower, S. Barnoy, Caspase-1 activity is required for neuronal differentiation of PC12 cells: Cross-talk between the caspase and calpain systems, Biochim. Biophys. Acta 1743 (2005) 223–230.
[29] K. Yamada, S. Senju, T. Nakatsura, Y. Murata, M. Ishihara, S. Nakamura, S. Ohno, A. Negi, Y. Nishimura, Identification of a novel autoantigen UACA in patients with panuveitis, Biochem. Biophys. Res. Commun. 280 (2001) 1169–1176.
[30] T. Sakai, L. Liu, X. Teng, R. Mukai-Sakai, H. Shimada, R. Kaji, T. Mitani, M. Matsumoto, K. Toida, K. Ishimura, Y. Shishido, T.W. Mak, K. Fukui, Nucling recruits Apaf-1/pro-caspase-9 complex for the induction of stress-induced apoptosis, J. Biol. Chem. 279 (2004) 41131–41140.
[31] L. Liu, T. Sakai, N. Sano, K. Fukui, Nucling mediates apoptosis by inhibiting expression of galectin-3 through interference with nuclear factor κB signaling, Biochem. J. 380 (2004) 31–41.